DOI 10.5012/bkcs.2011.32.8.2531

Articles

Photoemission Study on the Adsorption of Ethanol on Chemically Modified TiO_2(001) Surfaces

Ja Hyun Kong and Yu Kwon Kim*

Department of Energy Systems Research and Department of Chemistry, Ajou University, Suwon 443-749, Korea
**E-mail: yukwonkim@ajou.ac.kr*
Received June 7, 2011, Accepted June 11, 2011

Ethanol is a prototype molecule used in probing catalytic reactivity of oxide catalysts such as TiO_2. In the present study, we adsorbed ethanol on TiO_2(001) at room temperature (RT) and the corresponding bonding state of ethanol was systematically studied by x-ray photoemission spectroscopy (XPS) using synchrotron radiation. Especially, we compared TiO_2(001) surfaces prepared in ultra-high vacuum (UHV) with different surface treatments such as Ar^+-sputtering and oxidation with molecular O_2, respectively. We find that the saturation coverage of ethanol at RT varies depending on the amount of reduced surface defects (e.g., Ti^{3+}) which are introduced by Ar^+-sputtering. We also find that the oxidized TiO_2(001) surface has other type of surface defects (not related to Ti 3*d* state) which can dissociate ethanol for further reaction above 600 K. Our C 1*s* core level spectra indicate clearly resolved features for the two chemically distinct carbon atoms from ethanol adsorbed on TiO_2(001), showing the adsorption of ethanol proceeds without C-C bond dissociation. No other C 1*s* feature for a possible oxidized intermediate was observed up to the substrate temperature of 650 K.

Key Words : Photoemission spectroscopy, Adsorption, Ethanol, TiO_2(001)

Introduction

TiO_2 has been known as a potential photocatalyst not only for the oxidation of organic molecules[1,2] but also for the water-splitting reaction for the production of H_2.[3] For this reason, intense research effort has been made to understand the origin of the TiO_2-catalyzed reactions of simple molecules such as H_2O,[4-6] O_2,[7-10] alcohols,[11-13] and aldehydes.[14,15]

It has been found that defects on TiO_2 play a dominant role in the initial dissociation of such reactant molecules. In addition to Ti^{3+} interstitials in the bulk, TiO_2 has various kinds of surface defects such as oxygen vacancies[16,17] and oxygen adatoms,[9,10,18] which are reported to be reaction sites for H_2O,[5,9,10] O_2,[8,18] and alcohols.[11] Also, recent reports indicate that Ti^{3+} interstitials[19] in the subsurface region are important in a catalytic coupling reaction of aldehydes.[14,15]

Photoemission studies can provide an important information on the electronic nature of such intrinsic defects which appear as a distinct band-gap state located at 0.9 eV below Fermi level (E_F).[20,21] The Ti 3*d* character of the band-gap state is observed[21] and is generally related to the excess charge associated with defects near the surface region such as oxygen vacancies[17,21] and Ti^{3+} interstitials.[17,19]

Surface defects can be intentionally induced by various surface treatments in UHV. An atomically well-ordered TiO_2 surface can be prepared by a few cycles of sputtering and annealing to 900 K without any significant reduction. Ar^+-sputtering may be used to prepare a Ti^{3+}-rich TiO_2 surface due to a preferential removal of surface oxygen atoms under a mild sputtering condition. Also, the reduced Ti^{3+} subsurface defects can be removed by the interaction with molecular O_2 at RT.[19] A prolonged dose of O_2 (up to 1000 L) is reported to induce the band-gap state completely suppressed, which is attributed to oxidation of Ti^{3+} interstitials nearby the surface region.[19] Also, the dissociative adsorption of molecular oxygen over oxygen vacancies is known to produce another type of surface defect which is an oxygen adatom.[18]

The oxygen vacancy is reported to be a reaction site for the dissociative adsorption of ethanol.[11,22-24] On the oxygen vacancy, the adsorption of ethanol proceeds by breaking O-H bond to produce ethoxy (CH_3CH_2O-) bound to the oxygen vacancy and hydrogen bound to a neighboring bridge-bonded oxygen atom.[11,22-24] A further catalytic decomposition of such alkoxy species can occur above 600 K through various competing reaction channels such as dehydration (alkene), dehydrogenation (aldehydes) and recombinative desorption (alcohol) as has been studied for simple aliphatic alcohols such as ethanol[24,25] and propanol.[12,26]

In the present study, we aim to enhance our understanding on the interaction of ethanol with such defects on a well-defined model oxide catalyst such as rutile TiO_2(001) using photoemission spectroscopy. While the oxygen vacancy is generally accepted to be a reaction site for the dissociative adsorption of ethanol, the role of other types of defects are not well-understood. To gain further insight into the role of

such defects on the catalytic reactivity of TiO_2, we compare the adsorption property of ethanol on $TiO_2(001)$ surfaces with various kinds of surface defects. The new insight gained from the present study is that the saturation coverage of ethanol at RT depends on the amount of reduced Ti^{3+} surface defects. While no oxidized intermediate is found from the RT adsorption of ethanol on our $TiO_2(001)$ surfaces, the saturation coverage of ethanol at RT is found to be enhanced on the surface with high Ti^{3+} defect concentration. The oxidized $TiO_2(001)$ surface is depleted with the Ti^{3+} defects, but may have oxygen adatoms which are attributed to the reason for the increase of the maximum desorption temperature of ethanol. Our C 1*s* core level photoemission spectra also confirm that ethanol preserves its C-C bond on our $TiO_2(001)$ surfaces until it desorbs at around 600 K.

Experimental Details

A single crystal $TiO_2(001)$ substrate (0.5 mm thick, one-side polished, MTI) was cut into 5 mm × 10 mm in size and ceramic-glued on a thin Ta foil and was introduced into a UHV chamber attached 7B1 beamline[27] at Pohang Accelerator Laboratory (PAL). For a temperature measurement, K-type thermocouple was spot-welded on the edge of the Ta foil wrapped around the TiO_2 crystal. A well-ordered and clean $TiO_2(001)$ is prepared by a few cycles of Ar^+-sputtering at 1 keV and annealing at 900 K. A clean $TiO_2(001)$ surface showed very sharp integer spots in LEED pattern indicating a large atomically ordered domain structure has been obtained.

A fair amount of experimental and theoretical studies were reported to elucidate the atomic structure of the $TiO_2(001)$ surface.[28-31] While the detailed atomic structure may vary depending on the treatment condition, theoretical studies show that the ideal (001) surface has two kinds of surface species which are a four-fold Ti^{4+} and a twofold oxygen.[30] Due to the high surface free energy of the (001) facet compared to other facets, the $TiO_2(001)$ surface was reported to undergo a surface reconstruction where the oxygen moves outwards and the titanium moves inwards.[31] Annealing above 1000 K may induce low surface energy facets in which 5-fold Ti^{4+} may coexist with 4-fold Ti^{4+}.[29] Considering our experimental conditions, our clean $TiO_2(001)$ surface is expected to be composed of a reconstructed surface with a four-fold Ti^{4+} and a twofold oxygen.

For a systematic preparation of surface defects, oxidation of $TiO_2(001)$ surface was performed by backfilling the chamber with O_2 (99.999 %) using a variable leak valve up to an O_2 ambient pressure of 10^{-6} torr. A defective $TiO_2(001)$ surface was prepared by an Ar^+-sputtering ($P_{Ar} = 1 \times 10^6$ torr, $E_{Ar^+} = 1$ keV, I = 1 μA, t = 5 min) at RT.

Ethanol was further purified by repeated freeze-pump-saw cycles prior to use and was dosed onto the TiO_2 substrate by backfilling the UHV chamber using a variable leak valve while the substrate was kept at RT.

XPS measurements were performed at the 7B1 beamline. Photoemission spectra of Ti 2*p*, O 1*s*, and C 1*s* core levels were taken using a commercial electron analyzer (PHOIBOS 150, SPECS) at a fixed normal emission at RT. Photon energies used for the measurement of Ti 2*p*, C 1*s* and valence band were 580 eV, 335 eV and 55 eV, respectively. The binding energies of the photoemission spectra were determined by the position of the Fermi edge of Ta foil in contact with the TiO_2 substrate. The C 1*s* core level spectra are carefully analyzed using a standard nonlinear least-squares fitting procedure with Voigt functions.[32]

Results and Discussion

We compare Ti 2*p* core level and valence band spectra of our three $TiO_2(001)$ surfaces, which are an atomically ordered $TiO_2(001)$, an oxidized $TiO_2(001)$, and Ar^+-sputtered $TiO_2(001)$ surfaces in Figure 1 and Figure 2, respectively. As shown in Figure 1, the Ti 2*p* core level from TiO_2 is characterized by the main Ti $2p_{3/2}$ peak at 459 eV, which is assigned to Ti^{4+} species in the TiO_2 lattice.[33-35] Both the clean and the oxidized $TiO_2(001)$ surfaces show a well-distinguished single peak at 459 eV, suggesting Ti^{4+} from a stoichiometric TiO_2 lattice is a dominant feature for both surfaces. A detailed comparison between the two surfaces show a minor shoulder feature (indicated by arrow) on the lower binding energy side of the main Ti $2p_{3/2}$ peak on the clean $TiO_2(110)$ surface. This minor low-binding energy feature may be attributed to a reduced Ti^{3+} species near the surface region. It has been reported that the RT oxidation of $TiO_2(110)$ decreases the population of Ti^{3+} interstitials in the subsurface region.[19] On the Ar^+-sputtered $TiO_2(001)$, the Ti $2p_{3/2}$ peak becomes even more pronounced toward lower

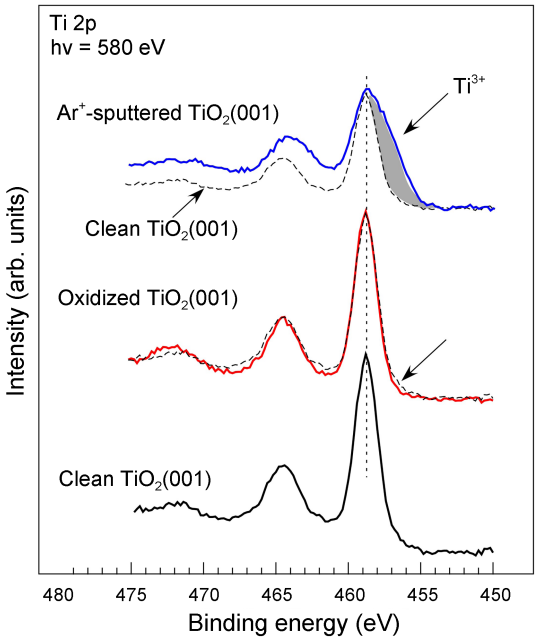

Figure 1. Ti 2*p* core level spectra taken from clean, oxidized, and Ar^+-sputtered $TiO_2(001)$ surfaces. Enhanced population of reduced Ti^{3+} state on the lower binding energy side of Ti $2p_{3/2}$ peak is indicated by arrows.

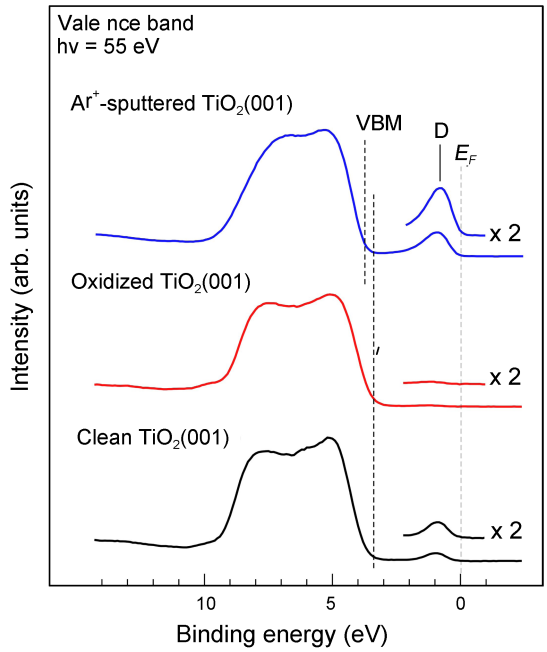

Figure 2. Valence band spectra taken from clean, oxidized, and Ar^+-sputtered TiO_2(001) surfaces. The band-gap state (D) varies on the three surfaces and reflects the population of Ti 3*d* state associated with surface defects such as oxygen vacancies and Ti^{3+} interstitials.

binding energy due to an enhanced population of Ti^{3+} species on the surface.

The variation of Ti^{3+}-related surface defects on the three surfaces is further examined in the valence band spectra in Figure 2. The broad feature at 3-9 eV is associated with O 2*p* state of TiO_2.[20,36] In addition, the distinct feature (D) at 0.9 eV below E_F is named the band-gap state and is associated with Ti 3*d* state.[20] The clean TiO_2(001) surface prepared in UHV shows a well-distinguished peak at 0.9 eV, while the state becomes completely suppressed on the oxidized TiO_2(001) surface. On the Ar^+-sputtered TiO_2(001) surface, the gap state is enhanced by three times compared to that on the clean surface. The magnitude of the band-gap state is related to the population of Ti^{3+} species (probably in the form of interstitials) on or near the surface region. In addition, a depletion of surface oxygen is noted from an attenuation in the O 2*p* state at 3 eV leading to an increase of the band gap. Thus, the results in Figure 1 and Figure 2 agree with each other and compare the relative population of Ti^{3+} species on the three TiO_2(001) surfaces.

Figure 3 shows C 1*s* core level spectra of ethanol adsorbed on the clean TiO_2(001) surface. The C 1*s* spectra taken after successively increasing ethanol dose of 5, 10, 20 L at RT (not shown here) indicate that the peak intensity does not increase above 5 L, suggesting that the RT saturation coverage is already achieved at the ethanol dose of 5 L. The two resolved peaks are attributed to the two chemically different carbon atoms of ethanol. Detailed fitting analysis (in Fig. 3) reproduces the two C 1*s* components positioned at 285.3 and 286.6 eV, respectively. The difference in the binding energies

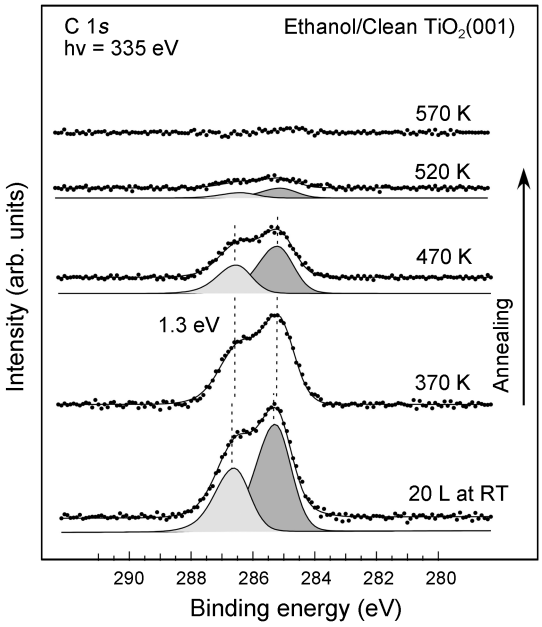

Figure 3. The C 1*s* core level spectra taken from ethanol adsorbed on the clean TiO_2(001) surface at RT up to a saturation coverage and after subsequent annealing to higher temperatures.

between the two components is measured to be about 1.3 eV. The peak shape is found to be asymmetric and has a tail toward higher binding energies due to the contribution of C-H vibrational satellite.[37] The peak at 285.3 eV is assigned to the β-carbon atom(-CH_3) and the peak at 286.6 eV to the α-carbon atom (-O-CH_2-).[26,38] The intensity ratio between the two peaks is measured to be 1.6-1.7 (which is far from 1), while we assume a one-to-one ratio in the populations of the two carbon atoms. We speculate the origin is related to

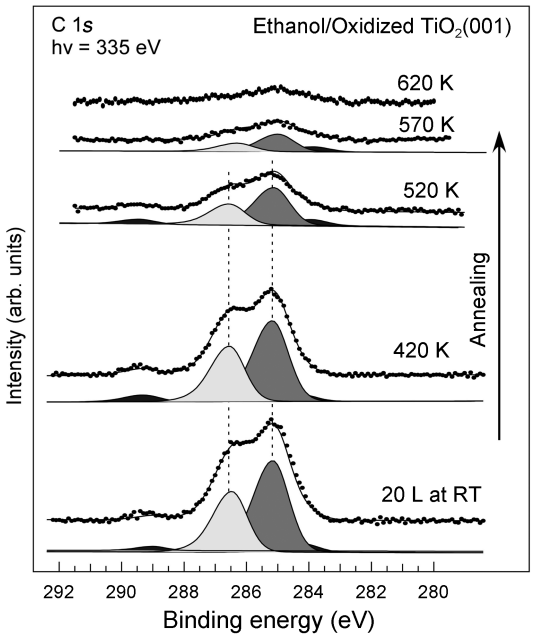

Figure 4. The C 1*s* core level spectra taken from ethanol adsorbed on the oxidized TiO_2(001) surface at RT up to a saturation coverage and after subsequent annealing to higher temperatures.

the bonding geometry of ethanol where ethanol is bonded to Ti^{4+} by its oxygen atom, thus makes the β-carbon (CH_3-) more surface-sensitive.

After successive annealing to higher temperatures, both C 1*s* peaks decrease gradually until they are completely removed by 570 K. The result agrees with earlier reports that ethanol adsorbs on TiO_2 either molecularly on Ti^{4+} sites[22,26] or dissociatively[22,24,26] on defect sites as an ethoxy (CH_3CH_2O-) and a hydrogen (-H). The catalytic decomposition of the ethoxy may occur at higher desorption temperatures (> 600 K) followed by desorption of reaction products. No other feature indicative of any oxidized intermediate is found.

Figure 4 shows the C 1*s* core level spectra for ethanol on the oxidized TiO_2(001) surface at RT as well as after subsequent annealing to higher temperatures. We find the two main C 1*s* components at 285.2 and 286.5 eV, respectively, which shows again the difference in the chemical shifts between the two components to be about 1.3 eV. In addition, we notice additional features at 289 eV and 284.3 eV, respectively. In fact, both features are not related to ethanol. Instead, they are attributed to a possible contamination introduced on the TiO_2 surface during prolonged O_2 dose up to 1000 L in our chamber since we observe the same features even after the RT oxidation of the TiO_2(001) surface. Thus, we disregard those features in our discussion.

After successive annealing to higher temperatures, we observe that both C 1*s* features gradually decrease with increasing annealing temperatures. We also note that the ethanol-related C 1*s* features at 285-286.5 eV persist even above 600 K.

The increase of the maximum desorption temperature on the oxidized TiO_2(001) surface is related to a stronger binding site which may involve surface defects such as an oxygen adatom, where a dissociative adsorption of ethanol may occur. On TiO_2(110), dissociative adsorption of ethanol is reported to leave ethoxy bound to oxygen vacancy on the surface.[23,24,39] After the hydroxyl hydrogen atoms (dissociated from ethanol) desorb from the surface as H_2O by 500 K, a recombinative ethanol desorption of ethoxy (left on the surface) is suppressed because no hydrogen is left on the surface by that temperature. Instead, catalytic decompositions of such ethoxy species are reported to occur on TiO_2(110) above 600 K.[22,24,26] We assume that oxygen vacancy is depleted on the oxidized surface due to dissociative adsorption of molecular oxygen, which would necessarily leave an oxygen adatom on the surface. We speculate that the C 1*s* species left after the annealing temperatures above 570 K is related to a dissociatively adsorbed ethoxy on a surface defect such as a low-coordinated oxygen adatom.

Figure 5 shows the C 1*s* core level spectra for ethanol on our Ar^+-sputtered TiO_2(001) surface at RT as well as after subsequent annealing to higher temperatures. We find again the two main C 1*s* components at 285.2 and 286.6 eV, respectively. Here, the difference in the chemical shifts between the two C 1*s* components is measured to be 1.4 eV. We defy any further discussion on the chemical shift difference between 1.3 and 1.4 eV considering the uncertainty in our peak position measurements (± 0.1 eV). After successive annealing to higher temperatures, we find again a gradual decrease of both C 1*s* peaks until they completely disappear by 570 K probably due to the desorption of ethanol.

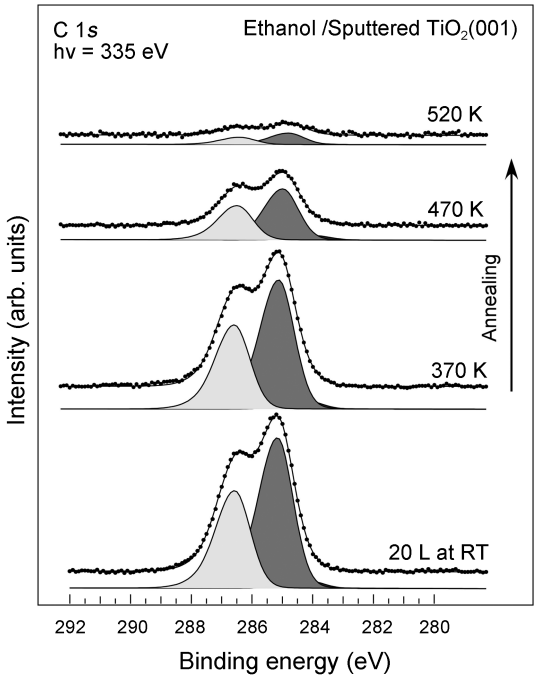

Figure 5. The C 1*s* core level spectra taken from ethanol adsorbed on the Ar^+-sputtered TiO_2(001) surface at RT up to a saturation coverage and after subsequent annealing to higher temperatures.

The integrated area of the two C 1*s* features at 285-286.5 eV may be used to estimate the amount of ethanol adsorbed on the TiO_2 surfaces. In Figure 6, we show our estimated number of ethanol molecules calculated by considering the sensitivity of C 1*s* core level compared to O 1*s* core level.

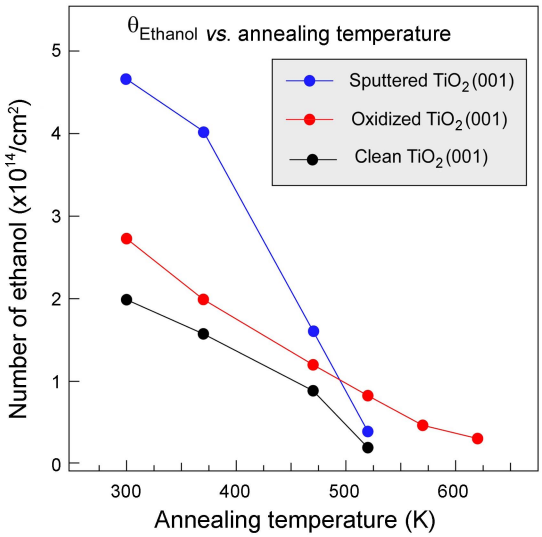

Figure 6. A variation in the amount of ethanol adsorbed on each TiO_2(001) surface at RT as the substrate temperature is raised to higher temperatures.

Due to a possible huge uncertainty associated with our estimation, we focus on the relative coverage of ethanol on the various TiO_2(001) surfaces. We note here that the initial saturation coverage of ethanol on sputtered TiO_2(001) is greatly enhanced compared to that on the clean and the oxidized TiO_2(001) surfaces.

Figure 6 also shows how the coverage of ethanol varies on the various TiO_2(001) surfaces at RT as well as after annealing to higher temperatures. Here, we find two noticeable trends: (1) On the clean and Ar^+-sputtered TiO_2(001) surfaces, the surface coverage of ethanol approaches to zero by 550 K, while that is extended to higher temperatures above 600 K on the oxidized TiO_2(001). (2) The initial saturation coverage of ethanol on the Ar^+-sputtered TiO_2(001) is higher than that on the clean surface.

The observation (1) gives an additional insight into the characteristics of the surface defect state of TiO_2(001). The fact that the desorption of ethanol completes by 550 K may suggest that there is no such defective site as oxygen vacancies on the clean TiO_2(001) surface since it is known that the dissociative adsorption of ethanol on the oxygen vacancy of TiO_2(110) is removed only above 600 K. While no oxygen vacancy is expected on the clean TiO_2(001), the valence band in Figure 2 shows the band-gap state suggesting the presence of Ti 3*d* state. Thus, the band-gap state is related to Ti^{3+} interstitials instead of oxygen vacancies on TiO_2(001).

The observation (2) suggests that the saturation coverage of ethanol at RT may be related to Ti^{3+} defects on the surface. The Ti 2*p* core level of the clean TiO_2(001) surface in Figure 1 shows that the dominant Ti species is in the form of Ti^{4+} instead of Ti^{3+} defects. In general, it is believed that the surface concentration of Ti^{3+} defects should be in equilibrium with that in the bulk (or subsurface) after the final annealing to 900 K. Thus, a major fraction of Ti^{3+} should be present in the subsurface and may have an influence on the binding of ethanol at RT. On the Ar^+-sputtered TiO_2(001), the excess Ti^{3+} defects on the surface are considered to be the origin of the increased saturation coverage of ethanol.

It is also interesting to note that the saturation coverage of ethanol on the oxidized surface is still comparable with that on the clean TiO_2(001) surface, while the valence band indicates that the Ti 3*d*-related defect state is completely suppressed on the oxidized surface. While it is largely unknown about the origin of surface defects on the oxidized TiO_2(001) surface, we tentatively attribute our results to the role of oxygen adatoms for a possible low-coordinated adsorption site, where ethanol may be dissociatively adsorbed. It requires however further experimental and theoretical studies to clearly address the exact origin of the binding interaction of ethanol on the oxidized TiO_2(001) surface.

Conclusions

Ethanol was used to probe the role of surface defects in the catalytic reactivity of TiO_2(001) surfaces. TiO_2(001) surfaces were prepared with various amounts of surface defects by a final annealing to 900 K, Ar^+-sputtering at RT and oxidation with O_2 at RT, respectively, while the nature of surface defects was characterized by measuring the Ti 2*p* core level and the valence band photoemission spectra. Our results indicate that the saturation coverage of ethanol at RT increases when the population of the reduced surface defects (e.g., Ti^{3+}) is increased. However, the maximum desorption temperature of ethanol is found to be unchanged with increased population of such reduced (Ti^{3+}) defects. Instead, the ethanol desorption temperature is observed to be extended to higher temperatures on the oxidized surface, where the reduced Ti^{3+} species are nearly depleted. We suggest that the origin of the stronger binding site for ethanol on the oxidized TiO_2(001) surface is related to a low-coordinated oxygen adatom on the surface.

Acknowledgments. This research was supported by Basic Science Research Program through the National Research Foundation of Korea (NRF) funded by the Ministry of Education, Science and Technology (2010-0010780) and by the new faculty research fund of Ajou University.

References

1. Diebold, U. *Surf. Sci. Rep.* **2003**, *48*, 53.
2. Wang, R.; Hashimoto, K.; Fujishima, A.; Chikuni, M.; Kojima, E.; Kitamura, A.; Shimohigoshi, M.; Watanabe, T. *Nature* **1997**, *388*, 431.
3. Fujishima, A.; Honda, K. *Nature* **1972**, *238*, 37.
4. Wendt, S.; Matthiesen, J.; Schaub, R.; Vestergaard, E. K.; Laegsgaard, E.; Besenbacher, F.; Hammer, B. *Phys. Rev. Lett.* **2006**, *96*, 066107.
5. Zhang, Z.; Bondarchuk, O.; Kay, B. D.; White, J. M.; Dohnalek, Z. *J. Phys. Chem. B* **2006**, *110*, 21840.
6. Li, S. C.; Zhang, Z.; Sheppard, D.; Kay, B. D.; White, J. M.; Du, Y.; Lyubinetsky, I.; Henkelman, G.; Dohnalek, Z. *J. Am. Chem. Soc.* **2008**, *130*, 9080.
7. Henderson, M. A.; Epling, W. S.; Perkins, C. L.; Peden, C. H. F.; Diebold, U. *J. Phys. Chem. B* **1999**, *103*, 5328.
8. Petrik, N. G.; Zhang, Z. R.; Du, Y. G.; Dohnalek, Z.; Lyubinetsky, I.; Kimmel, G. A. *J. Phys. Chem. C* **2009**, *113*, 12407.
9. Du, Y.; Deskins, N. A.; Zhang, Z.; Dohnalek, Z.; Dupuis, M.; Lyubinetsky, I. *Phys. Rev. Lett.* **2009**, *102*, 096102.
10. Zhang, Z.; Du, Y.; Petrik, N. G.; Kimmel, G. A.; Lyubinetsky, I.; Dohnalek, Z. *J. Phys. Chem. C* **2009**, *113*, 1908.
11. Zhang, Z. R.; Bondarchuk, E.; Kay, B. D.; White, J. M.; Dohnalek, Z. *J. Phys. Chem. C* **2007**, *111*, 3021.
12. Bondarchuk, O.; Kim, Y. K.; White, J. M.; Kim, J.; Kay, B. D.; Dohnalek, Z. *J. Phys. Chem. C* **2007**, *111*, 11059.
13. Kim, Y. K.; Kay, B. D.; White, J. M.; Dohnalek, Z. *Catal. Lett.* **2007**, *119*, 1.
14. Benz, L.; Haubrich, J.; Quiller, R. G.; Jensen, S. C.; Friend, C. M. *J. Am. Chem. Soc.* **2009**, *131*, 15026.
15. Benz, L.; Haubrich, J.; Quiller, R. G.; Friend, C. M. *Surf. Sci.* **2009**, *603*, 1010.
16. Zhang, Z.; Ge, Q.; Li, S. C.; Kay, B. D.; White, J. M.; Dohnalek, Z. *Phys. Rev. Lett.* **2007**, *99*, 126105.
17. Yim, C. M.; Pang, C. L.; Thornton, G. *Phys. Rev. Lett.* **2010**, *104*, 036806.
18. Du, Y.; Dohnalek, Z.; Lyubinetsky, I. *J. Phys. Chem. C* **2008**, *112*, 2649.
19. Wendt, S.; Sprunger, P. T.; Lira, E.; Madsen, G. K. H.; Li, Z. S.;

Hansen, J. O.; Matthiesen, J.; Blekinge-Rasmussen, A.; Laegsgaard, E.; Hammer, B.; Besenbacher, F. *Science* **2008**, *320*, 1755.
20. Henrich, V. E.; Dresselhaus, G.; Zeiger, H. J. *Phys. Rev. Lett.* **1976**, *36*, 1335.
21. Kurtz, R. L.; Stock-Bauer, R.; Madey, T. E.; Roman, E. L.; De Segovia, J. L. *Surf. Sci.* **1989**, *218*, 178.
22. Gamble, L.; Jung, L. S.; Campbell, C. T. *Surf. Sci.* **1996**, *348*, 1.
23. Kim, Y. K.; Kay, B. D.; White, J. M.; Dohnalek, Z. *Surf. Sci.* **2008**, *602*, 511.
24. Kim, Y. K.; Kay, B. D.; White, J. M.; Dohnalek, Z. *J. Phys. Chem. C* **2007**, *111*, 18236.
25. Campbell, C. T. *Surf. Sci. Rep.* **1997**, *27*, 1.
26. Farfan-Arribas, E.; Madix, R. J. *J. Phys. Chem. B* **2002**, *106*, 10680.
27. Hwang, H. N.; Kim, H. S.; Kim, B.; Hwang, C. C.; Moon, S. W.; Chung, S. M.; Jeon, C.; Park, C. Y.; Chae, K. H.; Choi, W. K. *Nucl. Instrum. Methods Phys. Res. A* **2007**, *581*, 850.
28. Mason, C. G.; Tear, S. P.; Doust, T. N.; Thornton, G. *J. Phys. Condens. Matt.* **1991**, *3*, S97.
29. Ariga, H.; Taniike, T.; Morikawa, H.; Tada, M.; Min, B. K.; Watanabe, K.; Matsumoto, Y.; Ikeda, S.; Saiki, K.; Iwasawa, Y. *J. Am. Chem. Soc.* **2009**, *131*, 14670.
30. Perron, H.; Domain, C.; Roques, J.; Drot, R.; Simoni, E.; Catalette, H. *Theor. Chem. Acc.* **2007**, *117*, 565.
31. Ramamoorthy, M.; Vanderbilt, D.; King-Smith, R. D. *Phys. Rev. B* **1994**, *49*, 16721.
32. Kim, Y. K.; Lee, M. H.; Yeom, H. W. *Phys. Rev. B* **2005**, *7111*, 5311.
33. Palgrave, R. G.; Payne, D. J.; Egdell, R. G. *J. Mater. Chem.* **2009**, *19*, 8418.
34. Takahashi, I.; Payne, D. J.; Palgrave, R. G.; Egdell, R. G. *Chem. Phys. Lett.* **2008**, *454*, 314.
35. Nambu, A.; Graciani, J.; Rodriguez, J. A.; Wu, Q.; Fujita, E.; Fdez Sanz, J. *J. Chem. Phys.* **2006**, *125*, 094706.
36. Tait, R. H.; Kasowski, R. V. *Phys. Rev. B* **1979**, *20*, 5178.
37. Kempgens, B.; Kivimaki, A.; Itchkawitz, B. S.; Koppe, H. M.; Schmidbauer, M.; Neeb, M.; Maier, K.; Feldhaus, J.; Bradshaw, A. M. *J. Electron. Spectrosc. Relat. Phenom.* **1998**, *93*, 39.
38. Jayaweera, P. M.; Quah, E. L.; Idriss, H. *J. Phys. Chem. C* **2007**, *111*, 1764.
39. Bondarchuk, O.; Huang, X.; Kim, J.; Kay, B. D.; Wang, L. S.; White, J. M.; Dohnalek, Z. *Angew. Chem.* **2006**, *45*, 4786.